Calcium phosphate preservation of faecal bacterial negative moulds in hyaena coprolites

MARÍA DOLORES PESQUERO, VIRGINIA SOUZA-EGIPSY, LUIS ALCALÁ, CARMEN ASCASO, and YOLANDA FERNÁNDEZ-JALVO

Pesquero, M.D., Souza-Egipsy, V., Alcalá, L., Ascaso, C., and Fernández-Jalvo, Y. 2014. Calcium phosphate preservation of faecal bacterial negative moulds in hyaena coprolites. *Acta Palaeontologica Polonica* 59 (4): 997–1005.

The vertebrate fossil locality of La Roma 2, Spain (Upper Miocene, Late Vallesian, MN10) is characterised by a high abundance of mammalian coprolites, which provide direct clues to the diets and habitats of the organisms that produced them. X-ray diffraction analysis showed a sample of hyaena (cf. *Lycyaena chaeretis*) coprolites to be mostly composed of calcium phosphate. Ultrastructural SEM and TEM studies revealed three successive phases of preservation, including an initial phase of mineralisation that produced microspherulites within a very fine-grained cement. This indicates that most of the calcium phosphate present in the coprolites precipitated rapidly, which in turn facilitated the formation of negative moulds of faecal bacteria within the coprolite matrix.

Key words: Bacteria, hyaena coprolites, structural preservation, taphonomy, Miocene, Spain.

María D. Pesquero [pesquero@fundaciondinopolis.org], Fundación Conjunto Paleontológico de Teruel-Dinópolis, 44002 Teruel, Spain; Museo Nacional de Ciencias Naturales, MNCN-CSIC, 28006 Madrid, Spain;
Virginia Souza-Egipsy [virginia.souza@ica.csic.es], Instituto de Ciencias Agrarias, ICA-CSIC, 28006 Madrid, Spain;
Luis Alcalá [alcala@fundaciondinopolis.org], Fundación Conjunto Paleontológico de Teruel-Dinópolis, 44002 Teruel, Spain;
Carmen Ascaso [ascaso@ccma.csic.es] and Yolanda Fernández-Jalvo [yfj@mncn.csic.es], Museo Nacional de Ciencias Naturales, MNCN-CSIC, 28006 Madrid, Spain.

Received 22 June 2012, accepted 15 February 2013, available online 19 February 2013.

Introduction

Lithified coprolites are irregular masses of mineralised soft material, which sometimes contain residues that shed light on ancient diets, trophic relationships and digestive efficiencies, as well as the mechanisms of soft-tissue preservation and diagenesis (Chin 2007). A variety of inclusions may be found inside coprolites, such as pollen, spores, phytoliths and other microfossils that provide information about the environment in which the producing animal lived. In addition, they also offer valuable insights into past ecosystems (Carrión et al. 2000, 2001, 2007; Scott et al. 2003; Prasad et al. 2005; Yll et al. 2006; Farlow et al. 2010; Fernández-Jalvo et al. 2010; Bon et al. 2012).

Apart from offering clues to the biology of the producer, coprolites also represent an excellent preservation medium for non-mineralised organisms, such as faecal bacteria. Bradley (1946) first reported minute particles of silica with bacterial morphologies from carnivore coprolites. Later, Schmitz-Münker and Franzen (1988) described fossil microorganisms preserved in coprolites of vertebrate carnivores from the Eocene Messel Oil Shale in Germany. These microorganisms, thought to be mainly bacteria, form hemispheroidal colonies a few microns in diameter and preserved in calcium phosphate. So far, there is no consensus as to how such hemispheroids form (Goth 1990; Liebig 1998). Clark (1989) provided the first record of bacterial structures (approximately 1.5 μm in length and 0.5 μm in diameter) in a coprolite of a conodontophagous animal.

More recently, Hollocher et al. (2001) observed organic remnants of bacterial colonies in coprolites produced by large herbivorous dinosaurs from the Cretaceous Two Medicine Formation of north-western Montana, and hypothesised that such colonies play a role in the initiation of faecal mineralisation. Toporski et al. (2002) studied the fossilised soft tissues of a tadpole and an associated coprolite from the organic-rich, volcaniclastic, lacustrine Enspel sediments (Upper Oligocene, Germany). Both contained 0.5–1 μm-sized spheres and rod shapes, interpreted as the fossil remains of bacterial biofilms. Northwood (2005) was the first to identify cyanobacteria in an

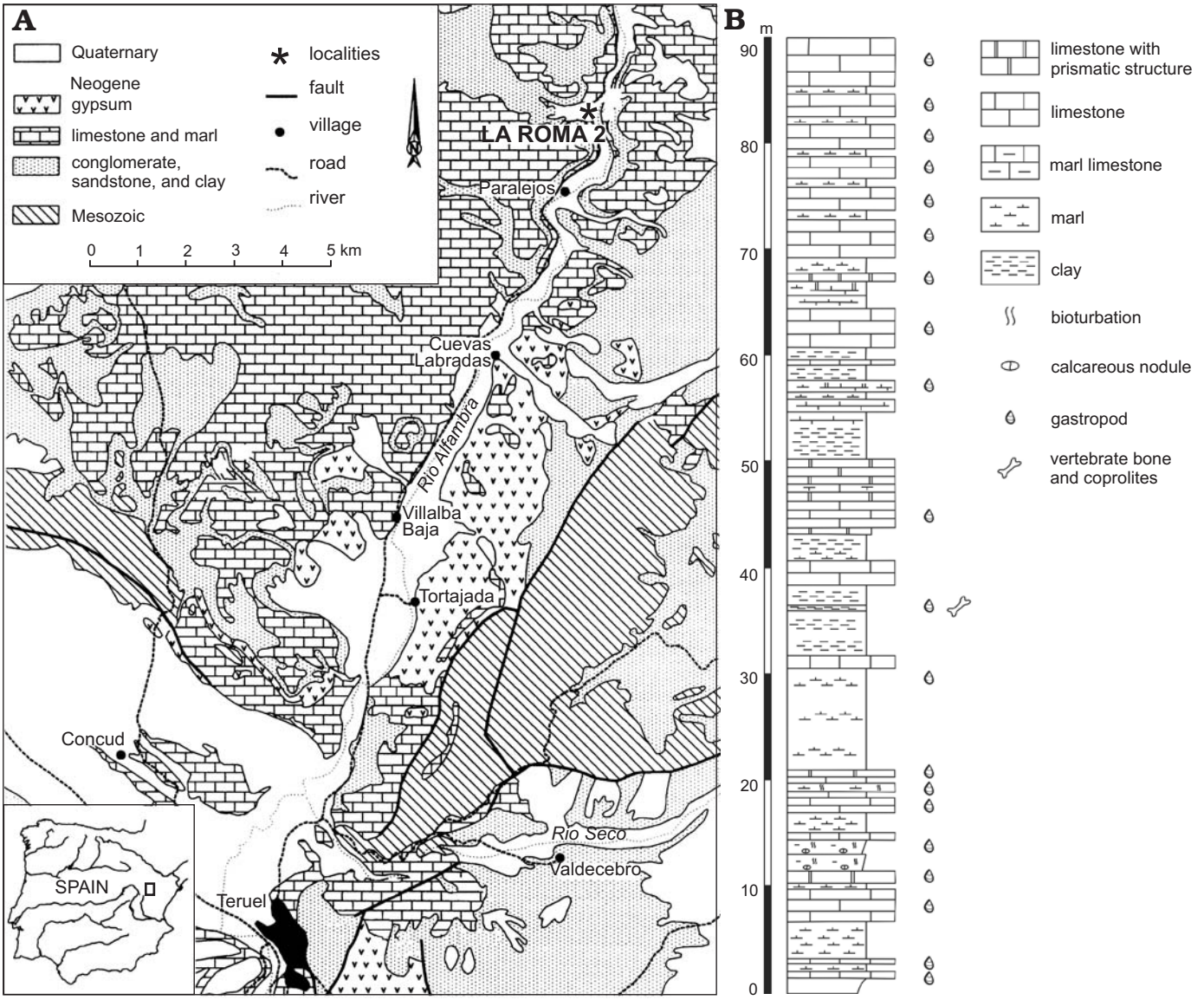

Fig. 1. **A**. Location of the La Roma 2 site (modified from van Dam et al. 2001). **B**. General stratigraphic section of the La Roma 2 site (modified from Alcalá 1994).

Early Triassic coprolite from the Arcadia Formation of Australia, thus demonstrating the value of coprolites as a preservation medium for non-mineralised organisms. Finally, Hollocher et al. (2010) described bacterial pseudomorphs from a carnivore coprolite, derived from a fluvial *Triceratops* site in the Upper Cretaceous Hell Creek Formation (USA). The authors ascribed the preservation of these delicate organic microstructures to rapid precipitation of dietary calcium phosphate, combined with a lack of diagenetic recrystallization thanks to rapid burial under anaerobic conditions.

In this study, we investigate the source, preservation, and post-depositional alteration of phosphatic coprolites from the locality of La Roma 2 (Upper Miocene, Spain), previously attributed to the Late Miocene hyaenid *Lycyaena chaeretis*, based on their size, shape and content (Pesquero et al. 2011). Using SEM–TEM tandem techniques, we furthermore provide detailed descriptions of organic inclusions and exceptionally well-preserved negative moulds of bacterial forms fossilised in the matrix.

Institutional abbreviations.—ICA, Instituto de Ciencias Agrarias, Madrid, Spain; MNCN, Museo Nacional de Ciencias Naturales, Madrid, Spain.

Geological setting

The site of La Roma 2 (Upper Miocene, Late Vallesian, MN10) is located in the north of the Teruel Basin (Spain), between the villages of Peralejos and Alfambra (Fig. 1A), and exposes a series of carbonate layers with a total thickness of 90 m (Fig. 1B). The fossiliferous level corresponds to a

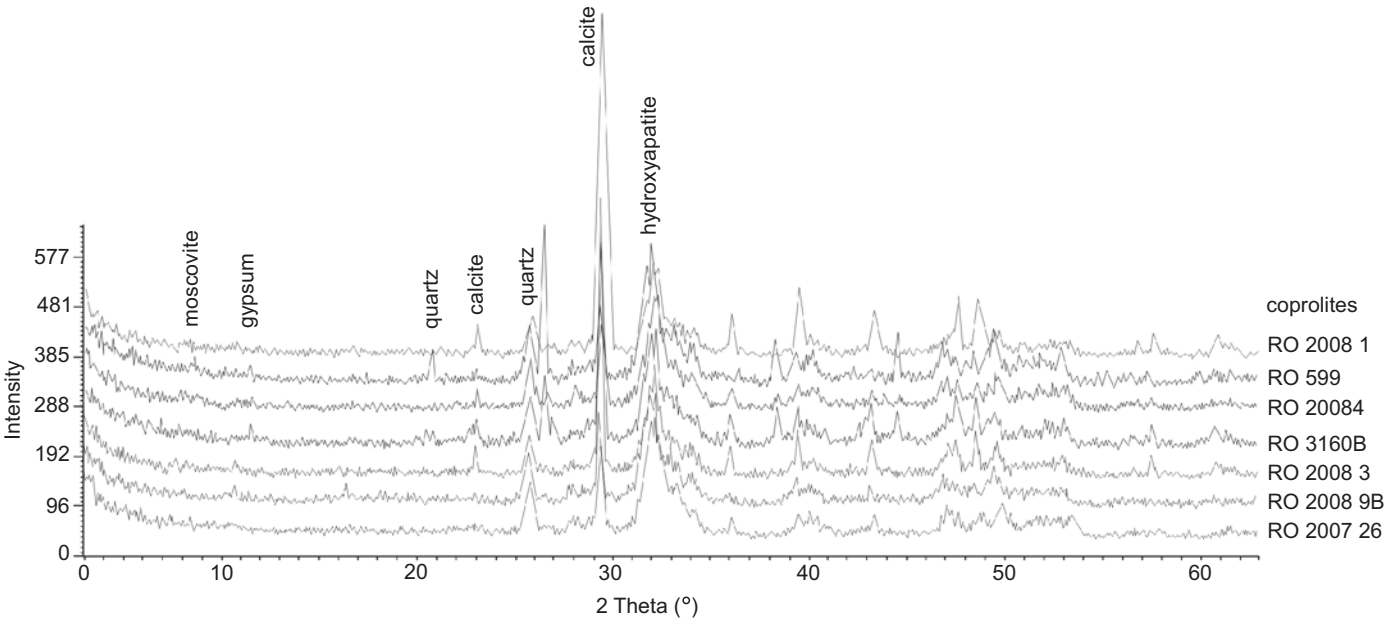

Fig. 2. X-Ray diffractograms of seven coprolites of the hyaenid *Lycyaena chaeretis* (Gaudry, 1861) from the locality of La Roma 2 (Upper Miocene, Spain). Image generated from XPowder Ver. 2004.04.46 PRO.

layer of grey clay marls representing an episodically flooded lakeshore, which saw the deposition of abundant organic material during times of high water levels. The mammalian remains found at the site were swept in and preserved under anoxic conditions. Previous taphonomic studies did not find any evidence for transport or sorting by high energy fluvial currents, but low energy streams may have reorganised the fossils after deposition (Cerdeño and Alcalá 1989; Alcalá et al. 1989–1990, 2011; van der Made et al. 1992; Acalá 1994; Alcalá and Morales 1997; Pesquero et al. 2006; Sánchez et al. 2009).

Material and methods

La Roma 2 has yielded more than 1000 mammalian carnivore coprolites, now held at the Museo Aragonés de Paleontología (Fundación Conjunto Paleontológico de Teruel-Dinópolis) in Teruel, Spain. We analysed six of these specimens: two by optical microscopy, one by transmission electron microscopy (TEM; LEO 910) and three by scanning electron microscopy (SEM; FEI Quanta 200) under both high and low vacuum conditions (Table 1). Two coprolites were embedded in epoxy resin, and transverse thin sections were cut for petrographic analysis under a Nikon Eclipse E-4000 POL petrographic microscope. For TEM, 1 mm^3 of the sample was vacuum-impregnated with low-viscosity Spurr's resin. Semithin (0.35 μm) and ultrathin sections (70–90 nm) were then prepared using an Ultracut E microtome (Reichert-Jung). The sections were then examined on copper grids with Pioloform film at 80 kV using the Electron Microscopy Service of ICA. For SEM, samples were gold sputter coated to obtain backscattered electron images using the electron microscopy facility of MNCN. EDS analyses were performed in 5 different spots in areas containing Na and Cl.

Seven samples were analysed by X-ray diffraction (powder method) to determine their mineralogical composition (Fig. 2). Of these, five were further analysed by X-ray fluorescence to determine their elemental composition (Table 2). Prior to taking the samples, the coprolites were cleaned and the outer layers removed. Samples were then taken from the interior of the coprolite, and crushed in an agate mortar and pestle. The analyses were performed using a Philips PW-1830 X-ray diffractometer and a Philips PW-1404 X-ray spectrometer. All samples were prepared and processed by the technicians at the sample preparation laboratory and the fluorescence and X-ray diffraction laboratory of MNCN.

Table 1. Samples analysed and techniques used. Abbreviations: diff., diffraction; EDS, energy dispersive spectroscopy; fluor., fluorescence; SEM, scanning electron microscopy; TEM, transmission electron microscopy.

Sample	SEM			TEM	Petrographic microscope	X-ray	
	surface	cut sections	EDS			diff.	fluor.
RO-SSC	×	×	×				
RO-599						×	
RO-2007-26						×	×
RO-2008-1	×	×	×			×	×
RO-2008-3	×	×	×			×	×
RO-2008-4						×	
RO-2008-9a					×		
RO-2008-9b					×	×	×
RO-2008-117				×			
RO-3160B						×	×

Results

Morphology and chemical composition.—The examined coprolites are mineralised and range between 23–80 mm in length and 20–45 mm in width, with a circular cross section and convex, concave, or pointed ends. At the fossil site, they formed part of a NNE-SSW band running subparallel to a band of fossil bones (for a more complete description, see Pesquero and Alcalá 2008). The spatial distribution of the coprolites and the lack of tooth marks on the nearby fossil bones suggest different provenances for these elements, and hence transport to their present positions by different water currents (Pesquero et al. 2011). However, hyaena droppings are very resistant (Larkin et al. 2000), and hence can retain their original shape and integrity even under such circumstances. A variety of inclusions are present inside the coprolites, including bone fragments, pollen grains and fungal spores, preserved in a microcrystalline matrix. All of the bone splinters show signs of corrosion, such as markedly rounded and polished edges, likely as a result of strong digestive processes. In terms of their composition, the coprolites contain mostly calcium phosphate (fluoro-hydroxyapatite) and calcite, with small amounts of quartz and gypsum (Fig. 2). CaO is the most abundant compound, followed by P_2O_5 (Table 2).

Thin section analysis.—The thin sections reveal a microcrystalline phosphatic matrix comprising three different zones (Fig. 3A): two outer zones, one with a homogenous (Zone X; Fig. 3B–E) and one with a heterogeneous texture (Zone Y; Fig. 3F–H); and a homogenously textured central zone characterised by secondary mineral deposition (Zone Z; Fig. 3D). In addition, there is a distinct, thin outer rim corresponding to the sticky surface of the dung (Fig. 3E). Zone X comprises a primary phosphatic matrix formed by microspherulites, whose original structure has been preserved by the surrounding fine-grained cement. In addition, there are small, calcite-coated circular voids, which were probably produced by gas bubbles arising from the digestive process. The margins of these voids show no trace of corrosion (Fig. 3C). By contrast, Zone Y shows greater degree of alteration, which likely reflects a post-depositional phase of mineralisation. This zone contains bone fragments within a microcrystalline matrix (Fig. 3F), as well as shrinkage cracks and irregular or oval voids coated by a thin, secondary patina of calcite crystals (Fig. 3H). The rounded voids probably originated from digestive processes, whereas the irregular ones likely represent additional shrinkage cracks produced when the coprolite lost volume during drying. Both the voids and shrinkage crack margins are deeply corroded, with iron oxide precipitation evident inside the primary hydroxyapatite matrix (Fig. 3G, H). Finally, Zone Z represents a tubular cavity filled with a microcrystalline hydroxyapatite matrix (Fig. 3D), and almost certainly was formed during the drying of the coprolite.

Electron microscopy.—SEM images of the voids in Zone X reveal the growth of calcite crystals towards the cavity (Fig. 4A). The matrix is composed of microspherulites ranging between 1–3 μm in diameter (Fig. 4B). A polished section analysed in backscattered detection mode shows these microspherulites to have two thin walls made of needle-shaped crystals (white arrows in Fig. 4C), suggesting an abiotic origin. The microspherulites are mostly embedded in a fine-grained calcium phosphate precipitate, with brighter areas indicative of enrichment in Na and Cl—probably from the liquids that circulated through the pore system of the coprolite after infiltrating it from the surrounding sediment (arrows in Fig. 4D; spectrum in Fig. 5).

At the highest magnification, spherical or elongated voids much smaller than the gas bubble cavities mentioned above become apparent in the fine mineral precipitate surrounding the microspherulites (Fig. 6A, white arrows in

Table 2. Chemical composition (percentage) of the coprolites determined by X-ray fluorescence. LOI: loss on ignition at 600ºC.

	RO-2007-26	RO-2008-1	RO-2008-3	RO-2008-9B	RO-3160B
Elements					
SiO_2	0.00	0.86	1.09	0.42	2.35
Al_2O_3	0.00	0.25	0.24	0.03	0.79
Fe_2O_3 (total)	0.00	0.00	0.00	0.00	0.00
MnO	0.00	0.00	0.00	0.00	0.00
MgO	0.33	0.66	0.56	0.53	0.60
CaO	44.7	49.37	46.7	44.37	44.12
Na_2O	0.14	0.32	0.23	0.39	0.30
K_2O	0.00	0.00	0.00	0.00	0.00
TiO_2	0.00	0.00	0.00	0.00	0.00
P_2O_5	37.48	30.20	31.55	36.16	31.78
LOI	15.2	16.10	17.6	16.25	17.49
Trace elements (ppm)					
Zr	–	–	–	–	–
Y	44	10	36	45	9
Rb	–	–	–	–	–
Sr	2741	1384	2298	1236	1386
Cu	–	–	–	–	–
Ni	5	–	4	21	–
Co	9	7	7	10	9
Ce	35	34	23	76	28
Ba	9527	2611	1683	220	2489
F	19386	18007	17877	16865	19432
S	7546	7044	7108	7209	7503
Cl	483	492	823	730	688
Cr	2	17	10	19	21
V	6	9	5	6	9
Th	1078	2146	153	327	2113
Nb	12	–	26	–	13
La	16	6	4	46	–
Zn	15	–	12	4	17
Cs	41	117	35	–	94
Pb	–	–	2	–	–

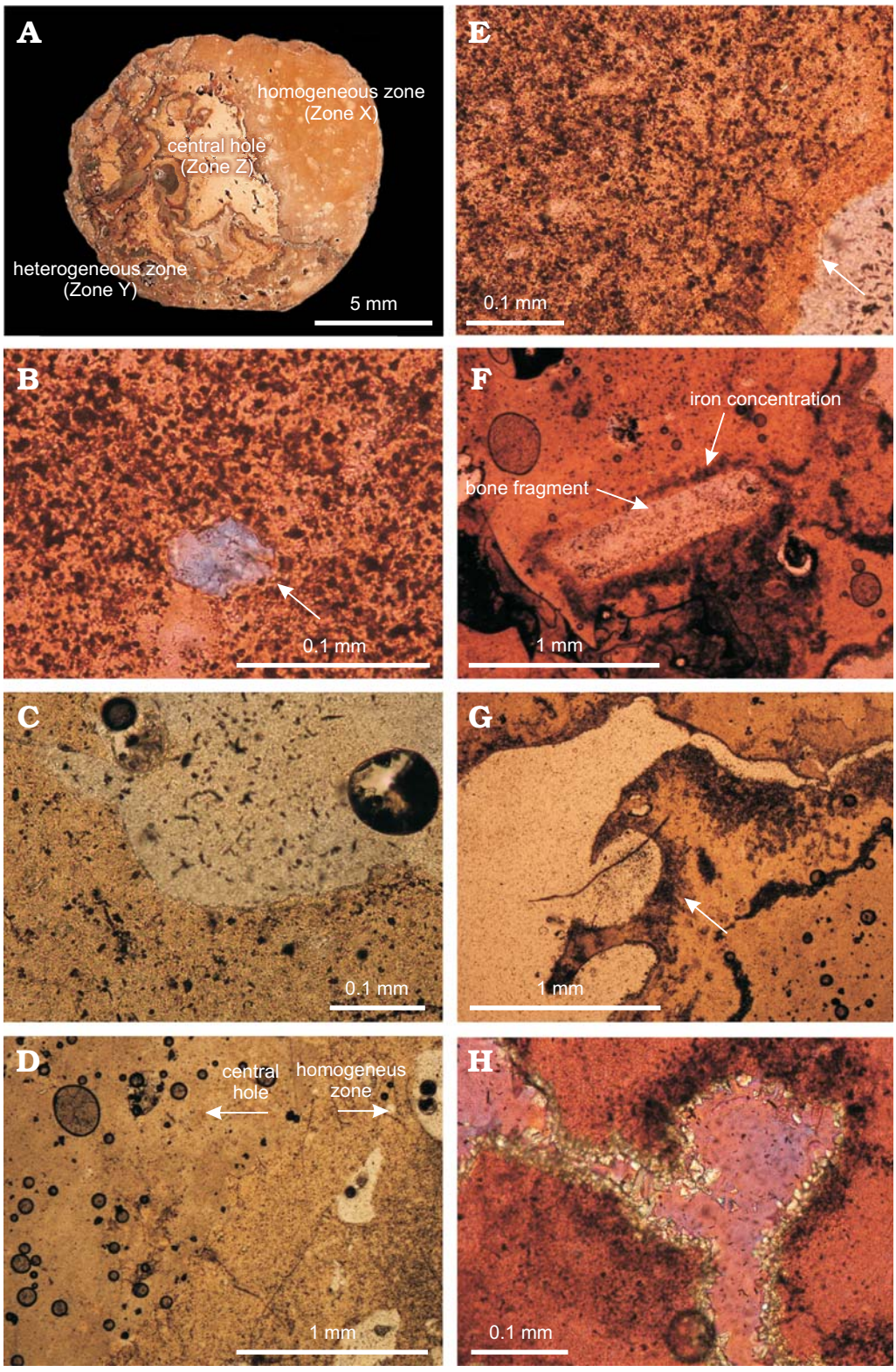

Fig. 3. Photomicrographs showing thin sections of a coprolite (RO-2008-9a) of the hyaenid *Lycyaena chaeretis* (Gaudry, 1861) from La Roma 2 (Upper Miocene, Spain). **A**. Section of the coprolite. **B**–**E**. Homogeneous zone (Zone X). **B**. Quartz inclusion, probably introduced from the surrounding sediment. **C**. A void, probably produced by gas, in the homogeneous zone (Zone X), with no filling and showing no corroded margins. **D**. Limit between the homogeneous zone (Zone X) (right) and the central hole (left) (Zone Z) (the rounded shapes are artefacts caused by the consolidation of the sample). **E**. Thin outer rim of the homogeneous zone (Zone X), showing a more compact phosphatic margin (orange, on the left). **F**–**H**. Heterogeneous zone (Zone Y). **F**. Bone fragment altered by digestive acids in the heterogeneous zone (Zone Y), showing the presence of iron in the surrounding phosphatic matrix. **G**. Voids and cracks within the heterogeneous zone (Zone Y), showing margin corrosion and iron precipitation partially replacing the original phosphatic matrix. **H**. Calcite-filled voids and shrinkage cracks in the heterogeneous zone (Zone Y).

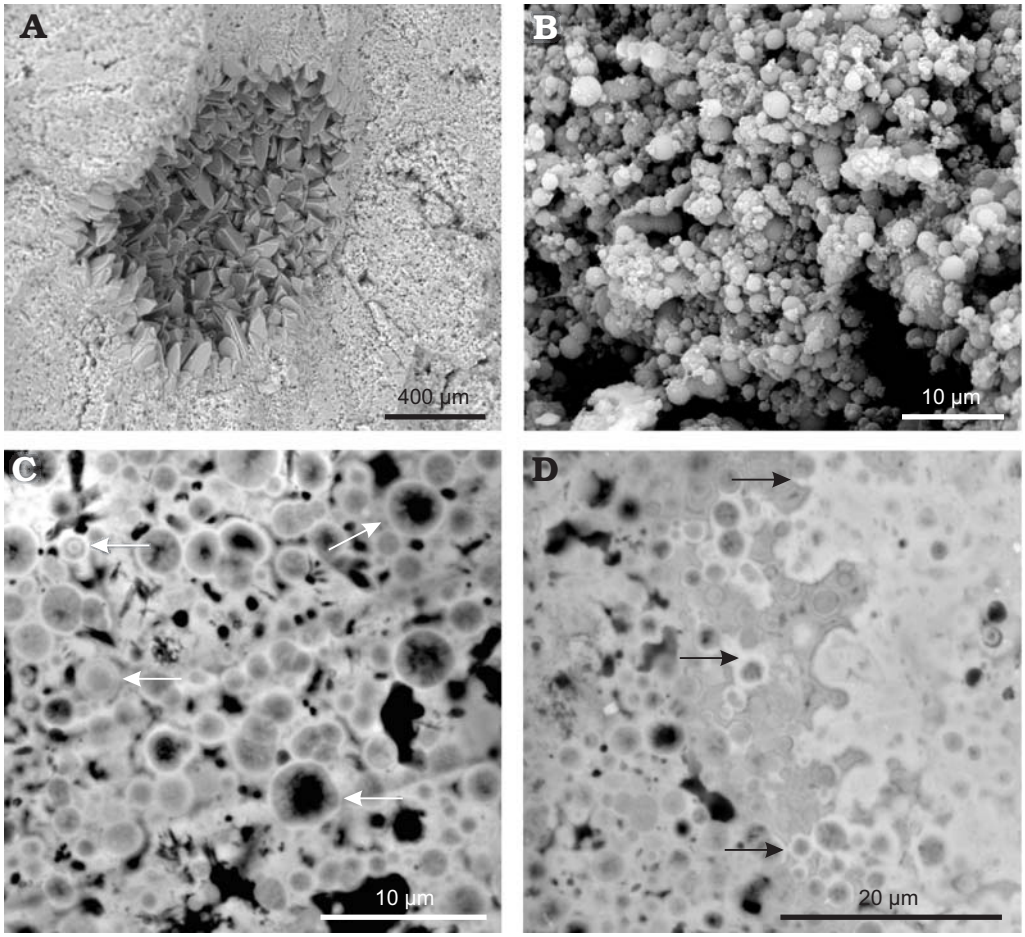

Fig. 4. SEM images of coprolites of the hyaenid *Lycyaena chaeretis* (Gaudry, 1861) from La Roma 2 (Upper Miocene, Spain). **A**. Calcite crystals inside a void likely produced by gas arising from digestive processes (RO-SSC). **B**. Matrix composed of microspherulites 1–3 µm in diameter (RO-SSC). **C**. Polished sections examined in backscattered detection mode, showing the thin-walled structure of the microspherulites (white arrows) (RO-2008-117). **D**. Microspherulites embedded in a fine-grained calcium phosphate precipitate; the brighter zones indicate areas enriched in Na and Cl (white arrows) (RO-2008-117).

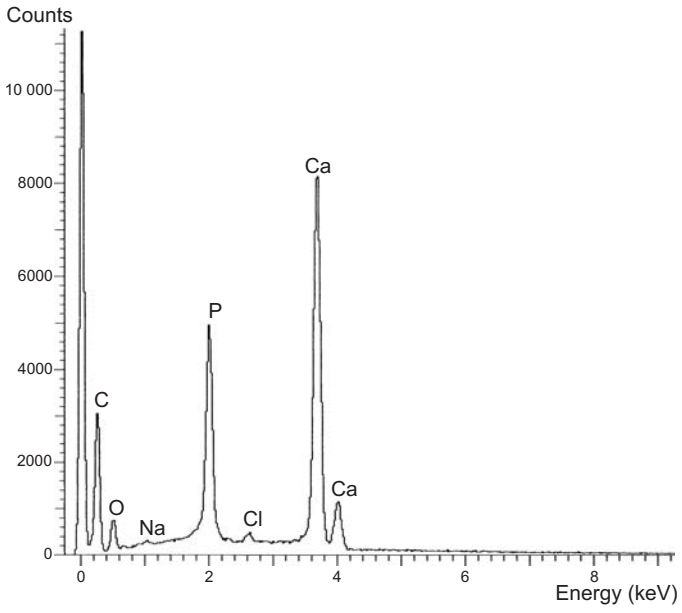

Fig. 5. EDS spectrum of the calcium phosphate matrix enriched in NaCl (Zone X) (RO-2008-117).

Fig. 6B, C). These micrometric voids resemble rod-shaped bacteria in both shape and size, as well as the fact that they are sometimes joined to each other at their extremes (white arrows in Fig. 6A–C). Similar voids, filled with resin and without any signs of compaction (as indicated by their smooth rims and nearly circular cross-sectional shape) are revealed by the TEM analysis of the ultrathin sections (arrows in Fig. 6D).

Discussion

Hyaena droppings are typically almost circular in cross section, with a concave end on one side and a more convex or occasionally pointed end on the other (Larkin et al. 2000). This morphology results from the peristaltic movement of the hyaenid digestive tract, and is highly characteristic. Another diagnostic feature of carnivore-produced coprolites is their high phosphate content. Hyaenas prey on large mammals and consume all parts of the body, although the horns, teeth and hair are usually later regurgitated (Kruuk 1975; Mills 1990; Larkin et al. 2000; Nowak 2005). The composition

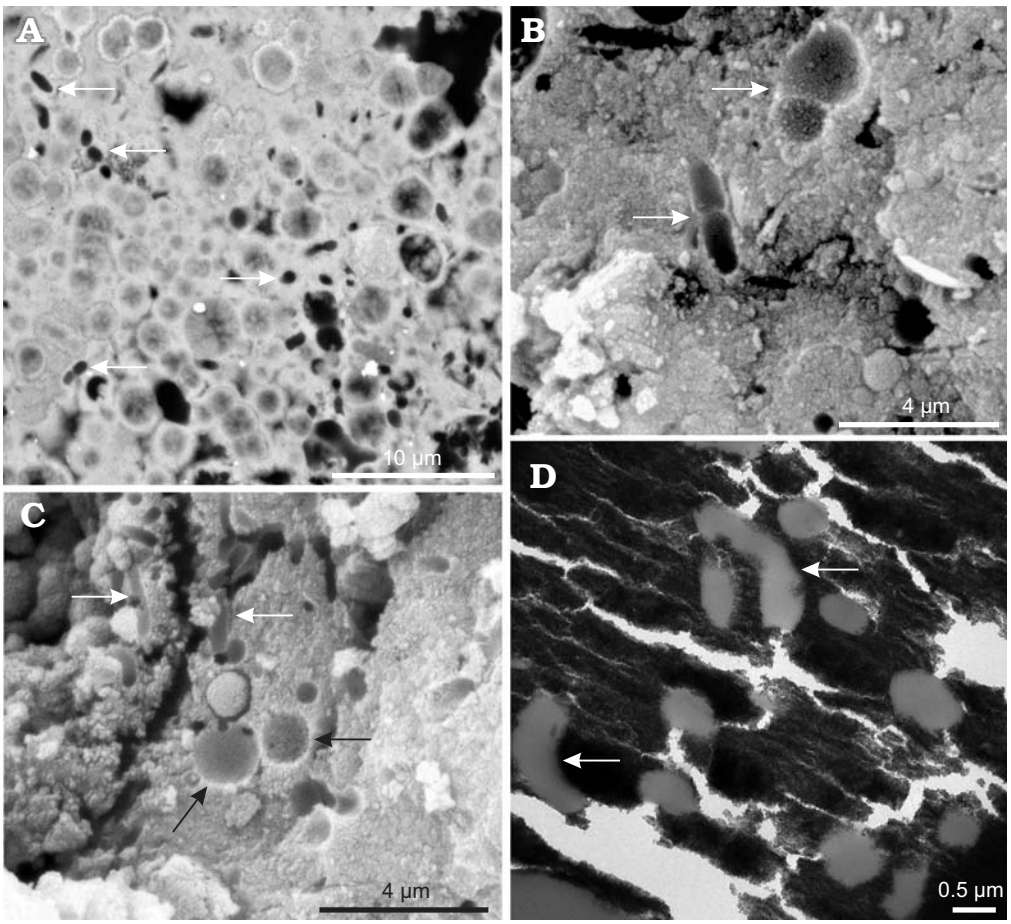

Fig. 6. SEM images of coprolites of the hyaenid *Lycyaena chaeretis* (Gaudry, 1861) from La Roma 2 (Upper Miocene, Spain). **A**. Spherical and elongated voids present in the fine calcium phosphate precipitated around the microspherulites (white arrows) (Zone X) (RO-2008-117). **B**, **C**. Small voids resembling rod-shaped bacteria (white arrows), differing from the microspherulites (black arrows) in their smaller size (RO-2008-3). **D**. TEM of an ultrathin section, showing negative moulds resembling rod-like bacteria (white arrows) in the fine calcium phosphate material (RO-2008-117).

of hyaena droppings is characterised by a large amount of $Ca_3(PO_4)_2Ca(OH)_2$, reflecting the ability of these animals to digest bone (Kruuk 1972; Larkin et al. 2000). The resulting high inorganic content of hyaenid coprolites renders their preservation more likely.

The size and shape of the coprolites studied here resemble excrements of the extant (*Crocuta crocuta*) and fossil spotted hyenas (Larkin et al. 2000; Fernández-Jalvo et al. 2010; Harrison 2010; Villa et al. 2010). In addition, the presence of bone splinters is consistent with their producers consuming substantial amounts of skeletal material. Isolated teeth of two species of hyaenid have been found at La Roma 2: the medium-sized *Hyaenictitherium* sp., which has a canid-like dentition; and the larger *Lycyaena chaeretis*, whose teeth are more suited to crushing. Both forms are considered cursorial meat and bone eaters (Turner et al. 2008; Werdelin and Solounias 1996). Given their size, the coprolites were more likely produced by *Lycyaena chaeretis*, which fits with the bone-crushing adaptations of this species (Pesquero et al. 2011).

The results of the mineralogical analysis provide an insight into the diagenetic history of the fossil site. Three phases of mineralisation can be identified. The first (Zone X) corresponds to a primary phosphatic matrix preserving the original structure of the coprolite (Fig. 3B–E). This indicates that the calcium phosphate precipitated soon after deposition, favouring the formation of faecal bacterial negative moulds. Alternatively, Zone X might represent the result of rapid, microbially-mediated lithification following burial (e.g., Chin et al. 2003); however, rapid precipitation of calcium carbonate before burial would have been more likely to protect the negative moulds of the faecal bacteria from potentially destructive changes resulting from groundwater chemistry. Post-burial recrystallisation during the second phase (Zone Y) erased the original morphology of the phosphatic matrix (Fig. 3F–H), although not all areas (i.e., Zone X) were equally affected (Chin 2007). It is possible that, following disruption of the initially homogeneous texture by early drying, exposure to mineral-bearing ground water may have caused Zone X to develop a relatively impermeable texture that was resistant to further alteration. Following burial, the coprolites underwent mineralogical changes caused by the infiltration of fluids enriched in carbonates and salt, suggesting a swampy environment similar to that surrounding the lake at La Roma 2. Finally, the third and last

phase saw the permineralisation of the central cavity (Zone Z), which likely originated during early shrinkage before lithification (Fig. 3D).

The micrometric, rod-shaped voids occurring around the microspherulites in Zone X strikingly resemble bacilliform bacteria in size and shape, and likely represent negative moulds of once-living bacterial cells (Fig. 6). By contrast, the origin of the microspherulites themselves is more obscure. Previous studies have shown that phosphatisation involving small apatite crystals can lead to exceptional tissue preservation (Briggs 2003; Briggs et al. 2005), thus raising the possibility that the microspherulites may represent mineralised microbes. On the other hand, experimental studies have successfully produced abiotic spherical apatite precipitates consisting of bundles of small crystallites (Busch et al. 1999) very similar to the ones in our specimens. Any biogenic origin of these microspherulites therefore remains questionable (Brasier et al. 2012).

Conclusions

We demonstrate three phases of mineralisation and the occurrence of well-preserved negative moulds of faecal bacteria, as well as potentially inorganic microspherulites, in Late Miocene hyaenid coprolites likely attributable to *Lycyaena chaeretis*. We find evidence of primary deposition of calcium phosphate similar to that seen in coprolites from the Upper Cretaceous Hell Creek Formation of North America. However, our material also underwent a phase of secondary mineralisation owing to the infiltration of their porous matrix by fluids enriched in carbonates and salts. These observations point to deposition in a swampy area, such as the margin of the lake known to have existed during the Vallesian in the La Roma 2 area.

Acknowledgements

We thank Amador Villamón (Mayor of Alfambra) and Carlos Bugeda (owner of the property where La Roma 2 is located), as well as the entire excavation and fossil preparation team for their cooperation. We also thank Laura Tormo and Marta Furió (Electron Microscopy Unit, MNCN) and Fernando Pinto (ICA) for their technical assistance. Karen Chin (University of Colorado, Boulder, CO, USA) and an anonymous reviewer provided critical reviews and valuable comments. This research was funded by the Dirección General de Patrimonio Cultural, Gobierno de Aragón (projects 02/92, 332/2006, 184/2007, 230/2008, 230/08/2009, and 230/08/09/2010), the Departamento de Educación, Cultura y Deporte, the Dirección General de Investigación, Innovación y Desarrollo, Gobierno de Aragón (Research Group E-62, FOCONTUR) and the Spanish Ministry of Science and Innovation (Project CGL2009-13903, Project CGL2010-19825, Projects CGL2010-16004 and CTM2009-12838-CO4-O3). MDP is a contracted researcher within the "Juan de la Cierva" programme (Ministerio de Ciencia e Innovación, ref. JCI-2007-132-565) at the Fundación Conjunto Paleontológico de Teruel-Dinópolis.

References

Alcalá, L. 1994. *Macromamíferos neógenos de la fosa de Alfambra-Teruel*. 554 pp. Instituto de Estudios Turolenses, Teruel.

Alcalá, L. and Morales, J. 1997. A primitive caprine from the Upper Vallesian of La Roma 2 (Alfambra, Teruel, Aragón, Spain). *Comptes Rendu de l'Academie de Sciences, Paris* 324: 947–953.

Alcalá, L., Morales, J., and Moyá, S. 1989–1990. El registro fósil neógeno de los bóvidos (Artiodactyla, Mammalia) de España. *Paleontologia i Evolució* 23: 67–73.

Alcalá, L., Pesquero, M.D., and Salesa, M. 2011. Hallazgo de hiracoideos en el área de Teruel. Nuevos datos sobre el Vallesiense de La Roma 2 (Alfambra). *Paleontologia i Evolució, memoria special* 5: 25–28.

Bon, C., Berthonaud, V., Maksud, F., Labadie, K., Poulain, J., Artiguenave, F., Wincker, P., Aury, J., and Elalouf, J. 2012. Coprolites as a source of information on the genome and dietof the cave hyena. *Proceedings of The Royal Society B: Biological Sciences* 279: 2825–2830.

Bradley, W.H. 1946. Coprolites from the Bridger Formation of Wyoming. Their composition and Microorganisms. *American Journal of Science* 244: 215–239.

Brasier, M.D. and Wacey, D. 2012. Fossils and astrobiology: new protocols for cell evolution in deep time. *International Journal of Astrobiology* 11: 217–228.

Briggs, D.E.G. 2003. The role of decay and mineralization in the preservation of soft-bodied fossils. *Annual Review of Earth and Planetary Sciences* 31: 275–301.

Briggs, D.E.G., Moore, R.A., Shultz, J.W., and Schweigert, G. 2005. Mineralization of soft-part anatomy and invading microbes in the horseshoe crab *Mesolimulus* from the Upper Jurassic Lagerstatte of Nusplingen, Germany. *Proceedings of the Royal Society B* 272: 627–632.

Busch, S., Dolhaine, H., DuChesne, A., Heinz, S., Hochrein, O., Laeri, F., Podebrad, O., Vietze, U., Weiland, T., and Kniep, R. 1999. Biomimetic morphogenesis of fluorapatite-gelatin composites: fractal growth, the question of intrinsic electric fields, core/shell assemblies, hollow spheres and reorganization of denatured collagen. *European Journal of Inorganic Chemistry* 1999: 1643–1653.

Carrion, J.S., Brink, J., Scott, L., and Binneman, J. 2000. Palynology of hyena coprolites from Oyster Bay, southeastern Cape coast, South Africa, the palaeo-environment of an open-air Howieson`s Poort occurrence. *South African Journal of Science* 96: 449–453.

Carrion, J.S., Riquelme, J.A, Navarro, C., and Munuera, M. 2001. Pollen in hyaena coprolites reflects late glacial landscape in southern Spain. *Palaeogeography, Palaeoclimatology, Palaeoecology* 176: 193–205.

Carrion, J.S., Scott, L., Arribas, A., Fuentes, N., Gil, G., and Montoya, E. 2007. Pleistocene landscapes in central Iberia inferred from pollen analysis of hyena coprolites. *Journal of Quaternary Science* 22: 191–202.

Cerdeño, E. and Alcalá, L. 1989. *Aceratherium alfambrense* n. sp., nuevo rinocerótido del Vallesiense superior de Teruel (España). *Revista Española de Paleontología* 4: 39–51.

Chin, K. 2007. Thin section analysis of lithified coprolites (fossil feces). *Microscopy and Microanalysis* 13: 504–505.

Chin, K., Eberth, D.A., Schweitzer, M.H., Rando, T.A., Sloboda, W.J., and Horner, J.R. 2003. Remarkable preservation of undigested muscle tissue within a Late Cretaceous tyrannosaurid coprolite from Alberta, Canada. *Palaios* 18: 286–294.

Clark, N.D.L. 1989. Carboniferous coprolitic bacteria from the Ardross Shrimp Bed, Fife. *Scottish Journal of Geology* 25: 99–104.

Farlow, J.O., Chin, K., Argast, A., and Poppy, S. 2010. Coprolites from The Pipe Creek Sonkhole (Late Neogene, Grant County, Indiana, U.S.A). *Journal of Vertebrate Paleontology* 30: 959–969.

Fernández-Jalvo, Y., Scott, L., Carrión, J.S., Gil-Romera, G., Brink, J., Neumann, F., and Rossouw, Ll. 2010. Pollen Taphonomy of hyaena coprolites: an experimental approach. *In*: E. Baquedano and J. Rosell (eds.), Actas de la 1ª Reunión de Científicos sobre cubiles de hiena (y otros grandes carnívoros) en los yacimientos arqueológicos de la Península Ibérica. *Zona Arqueológica* 13: 148–156.

Goth, K. 1990. Der Messeler Ölschiefer–Ein Algenlaminit. *Courier Forschungsinstitut Senckenberg* 131: 1–143.

Harrison, T. 2010. Coprolites: taphonomic and paleoecological implications. *In*: T. Harrison (ed.), *Paleontology and Geology of Laetoli: Human Evolution in Context, Volume 1: Geology, Geochronology and Paleoecology and Paleoenvironment*. 393 pp. Springer, Dordrecht.

Hollocher, T.C., Chin, K., Hollocher, K.T., and Kruge, M.A. 2001. Bacterial Residues in Coprolite of Herbivorous Dinosaurs: Role of Bacteria in Mineralization of Feces. *Palaios* 16: 547–565.

Hollocher, K.T., Hollocher, T.C., and Rigby, J.K. 2010. A phosphatic coprolite lacking diagenetic permineralization from the upper Cretaceous Hell Creek Formation, Northeastern Montana: importance of dietary calcium phosphate in preservation. *Palaios* 25: 132–140.

Kruuk, H. 1972. *The Spotted Hyaena: A Study of Predation and Social Behaviour*. 335 pp. University of Chicago Press, Chicago.

Kruuk, H. 1975. *Hyaena*. 80 pp. Oxford University Press, Oxford.

Larkin, N.R., Alexander, J., and Lewis, M.D. 2000. Using experimental studies of Recent faecal material to examine hyaena coprolites from the West Runton Freshwater Bed, Norfolk, U.K. *Journal of Archaeological Science* 27: 19–31.

Liebig, K. 1998. Fossil microorganisms from the Eocene Messel Oil Shale of Southern Hesse, Germany. *Kaupia* 7: 1–95.

Mills, M.G.L. 1990. *Kalahari hyaenas: Comparative Behavioural Ecology of Two Species*. 304 pp. Unwin Hyman, London.

Nowak, R.M. 2005. *Walker's Carnivores of the World*. 323 pp. The Johns Hopkins University Press, Baltimore.

Northwood, C. 2005. Early Triassic coprolites from Australia and their Palaeobiological significance. *Palaeontology* 48: 49–68.

Pesquero, M.D., Alberdi, M.T., and Alcalá, L. 2006. New species of *Hipparion* from La Roma 2 (Late Vallesian, Teruel, Spain): a study of the morphological and biometric variability of *Hipparion primigenium*. *Journal of Paleontology* 80: 346–356.

Pesquero, M.D. and Alcalá, L. 2008. Taphonomy of the Miocene mammal site of La Roma 2 (Teruel, Spain) revisited. *In*: J. Aguirre, J.C. Braga, A.G. Checa, M. Company, and F.J. Rodríguez-Tovar (eds.), *Taphos´08, Quinta reunión de Tafonomía y Fosilización, Third meeting on Taphonomy and Fossilization*, 88–89. Instituto Geológico y Minero de España and Universidad de Granada, Universidad de Granada, Granada.

Pesquero, M.D., Salesa, M.J., Espílez, E., Mampel, L., Siliceo, G., and Alcalá, L. 2011. An exceptionally rich hyaena coprolites concentration in the Late Miocene mammal fossil site of La Roma 2 (Teruel, Spain): taphonomical and palaeoenvironmental inferences. *Palaeogeography, Palaeoclimatology, Palaeoecology* 311: 30–37.

Prasad, V., Strömberg, C.A.E., Alimohammadian, H., and Sahni, A. 2005. Paleontology: Dinosaur coprolites and the early evolution of grasses and grazers. *Science* 310: 1177–1180.

Sánchez, I.M., Domingo, M.S., and Morales, J. 2009. New data on the Moschidae (Mammalia, Ruminantia) from the Upper Miocene of Spain (MN10–MN11). *Journal of Vertebrate Paleontology* 29: 567–575.

Scott, L., Fernández-Jalvo, Y., Carrión, J., and Brink, J. 2003. Preservation and interpretation of pollen in hyaena coprolitos: taphonomic observations from Spain and southern Africa. *Palaeontologia Africana* 39: 83–91.

Schmitz-Münker, M. and Franzen, J. 1988. Die Rolle von Bakteren im Verdauungstrakt mitteleozäner Vertebraten und ihr Beitrag zur Fossildiagenese und Evolution. *In*: J.L. Franzen, and W. Michaelis (eds.), Der eozäne Messelsee–Eocene Lake Missal. *Courier Forschungsinstitut Senckenberg* 107: 129–146.

Toporski, J.K.W., Steele, A., Westall, F., Avci, R., Martill, D.M., and McKay, D.S. 2002. Morphologic and spectral investigation of exceptionally well-preserved bacterial biofilms from the Oligocene Enspel formation, Germany. *Geochimica et Cosmochimica Acta* 66: 1773–1791.

Turner, A., Antón, M., and Werdelin, L. 2008. Taxonomy and evolutionary patterns in the fossil Hyaenidae of Europe. *Geobios* 41: 677–687.

van Dam, J.A., Alcalá, L., Alonso Zarza, A.M., Calvo, J. P., Garcés, M., and Krijgsman, W. 2001. The Upper Miocene mammal record from the Teruel-Alfambra region (Spain): the MN system and continental Stage/Age concepts discussed. *Journal of Vertebrate Paleontology* 21: 367–385.

van der Made, J., Montoya, P., and Alcalá, L. 1992. *Microstonyx* (Suidae, Mammalia) from the Upper Miocene of Spain. *Geobios* 25: 395–413.

Villa, P., Goñi, M.F.S., Bescós, G.C., Grün, R., Ajas, A., and Pimienta, J.C.G. 2010. The archaeology and paleoenvironment of an Upper Pleistocene hyena den: an integrated approach. *Journal of Achaeological Science* 37: 919–935.

Werdelin, L. and Solounias, N. 1996. The evolutionary history of hyaenas in Europe and western Asia during the Miocene. *In*: R.L. Bernor, V. Fahlbusch, and S. Rietschel (eds.), *Later Neogene European Biotic Evolution and Stratigraphic Correlation*, 290–306. Columbia University Press, New York.

Yll, R., Carrión, J.S., Marra, A.C., and Bonfiglio, L. 2006. Vegetation reconstruction on the basis of pollen in Late Pleistocene hyena coprolites from San Teodoro Cave (Sicily, Italy). *Palaeogeography, Palaeoclimatology, Palaeoecology* 237: 32–39.